

Supporting Information

A New Insight into the Reversal of Multidrug Resistance in Cancer by Polymeric Nanodrug

Huangyong Jiang, Dong Chen, Dongbo Guo, Yan Wu, Xin Jin* and
Xinyuan Zhu

School of Chemistry and Chemical Engineering, State Key Laboratory of Metal Matrix
Composites, Shanghai Jiao Tong University, 800 Dongchuan Road, Shanghai 200240,
P. R. China. E-mail: jxcindy@sjtu.edu.cn

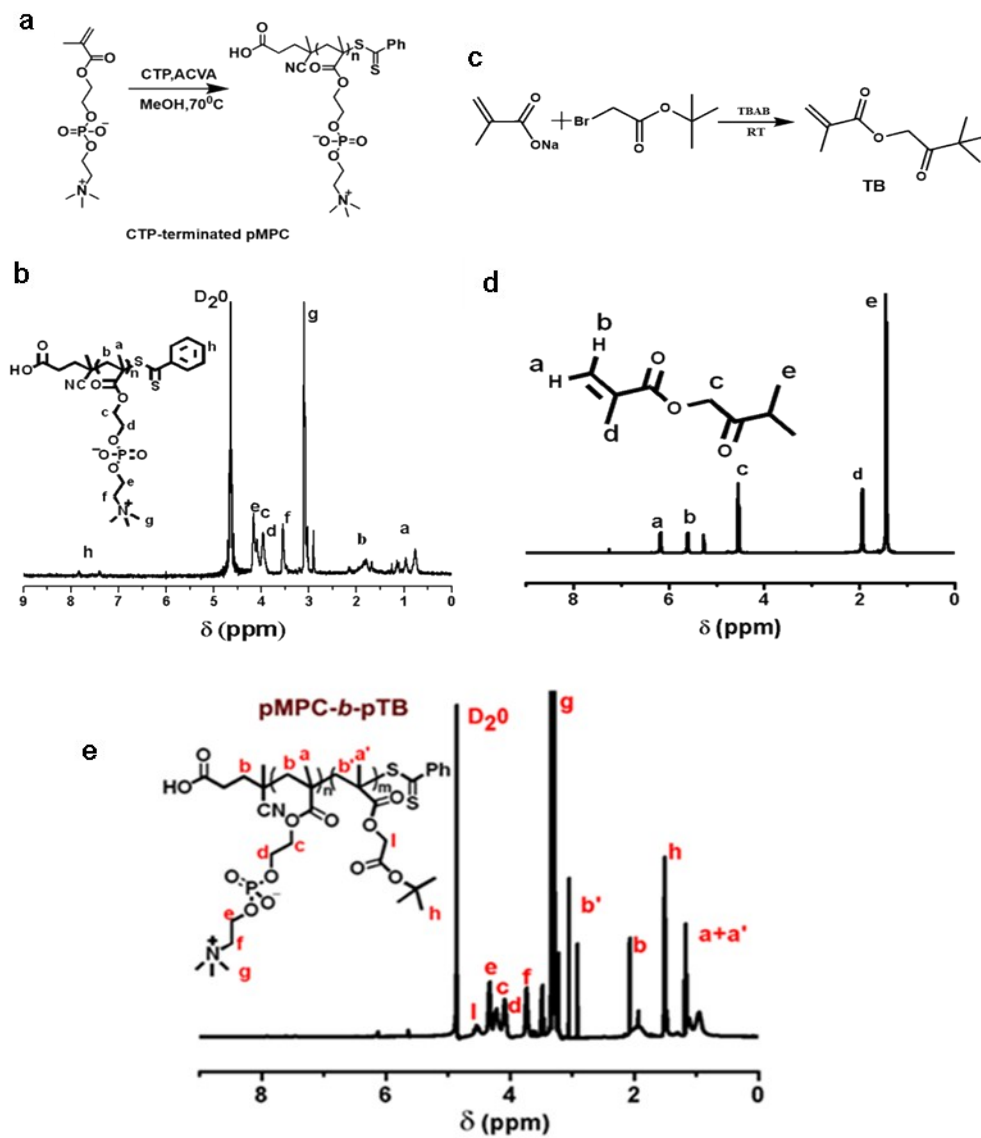


Figure S1: (a) Synthesis of macroRAFT agent (CTP-terminated pMPC). (b) ^1H NMR spectrum of CTP-terminated pMPC in D_2O . (c) Synthesis of monomer TB. (d) ^1H NMR spectrum of monomer TB in CDCl_3 . (e) ^1H NMR spectrum of CTP-terminated pMPC-*b*-pTB (BP) in D_2O .

Table S1. pMPC-*b*-pTB and the corresponding acyl hydrazide polymer

Polymer	Mw (KDa) ^a	PDI ^b	TBOEMA (mol %) ^c	Polymer	Mw (KDa)	PDI	Hydrazine (mol %) ^d
BP1	11	1.4	12%	BPN1	11	1.4	10%
BP2	13	1.6	22%	BPN2	12	1.7	21%
BP3	14	1.5	30%	BPN3	14	1.4	28%

^aMolecular weight measured by GPC. ^bPDI measured by GPC. ^cEstimated by ¹H NMR spectroscopy. ^dEstimated by ¹H NMR spectroscopy.

Table S2. Characterization of DOX-BP NPs.

samples	CMC values (mg/mL)	DOX (wt %) ^a	Size (DLS, nm) ^b	Size (TEM, nm) ^c	Zeta (mV) ^d
DOX-BP1	9.38×10^{-3}	10	~46	~33	0.02
DOX-BP2	1.18×10^{-2}	14	~136	~101	-0.01
DOX-BP3	1.35×10^{-2}	15	~225	~191	0.03

^aDOX loading is obtained by UV-vis spectroscopy at 488 nm. ^bHydrodynamic diameter measured in water by DLS. ^cNanoparticles sizes measured by TEM. ^dZeta potential measured in water by Zetasizer.

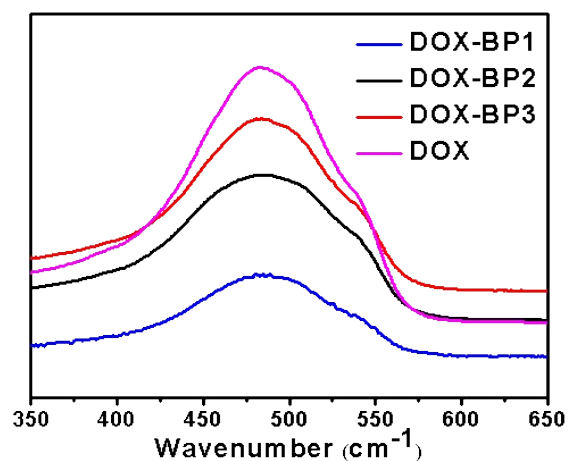


Figure S2: UV-vis spectrum of DOX-BP1, DOX-BP2, DOX-BP3 and DOX hydrochloride in water.

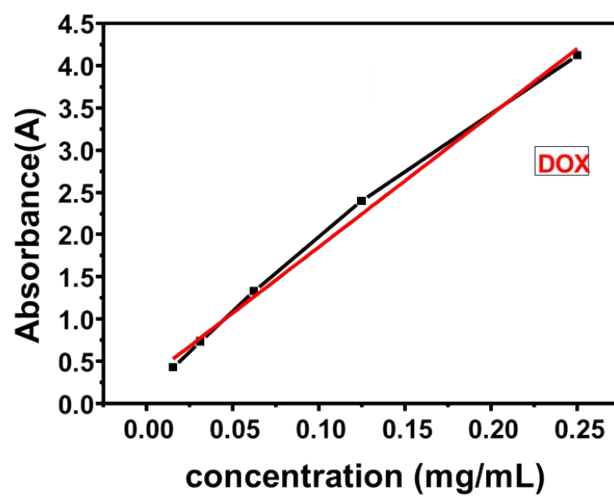


Figure S3: The standard curve of DOX hydrochloride in water at 480 nm.

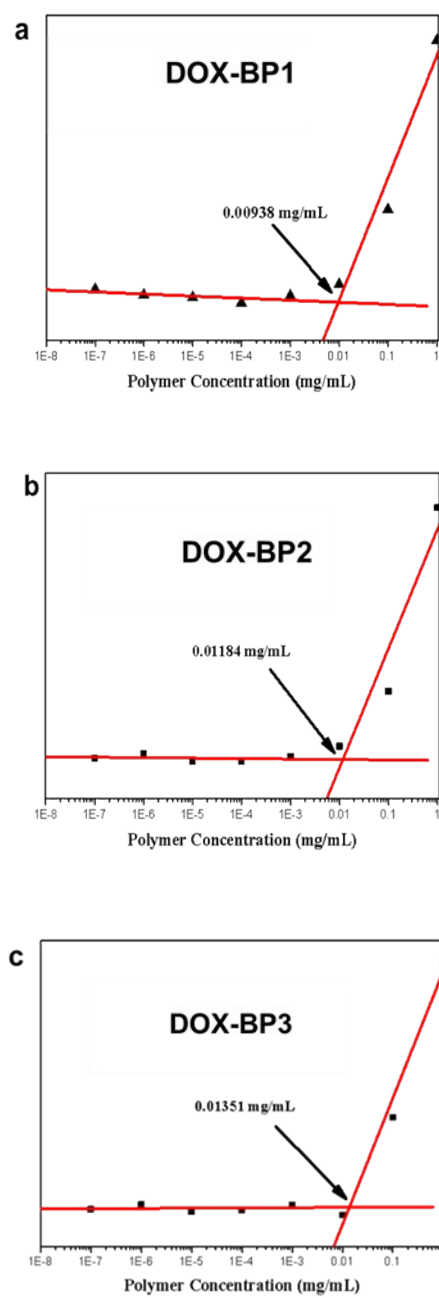


Figure S4: Emission intensity ($\lambda = 385$ nm) of Pyrene in an aqueous solution of a) DOX-BP1, b) DOX-BP2 and c) DOX-BP3 with various concentrations.

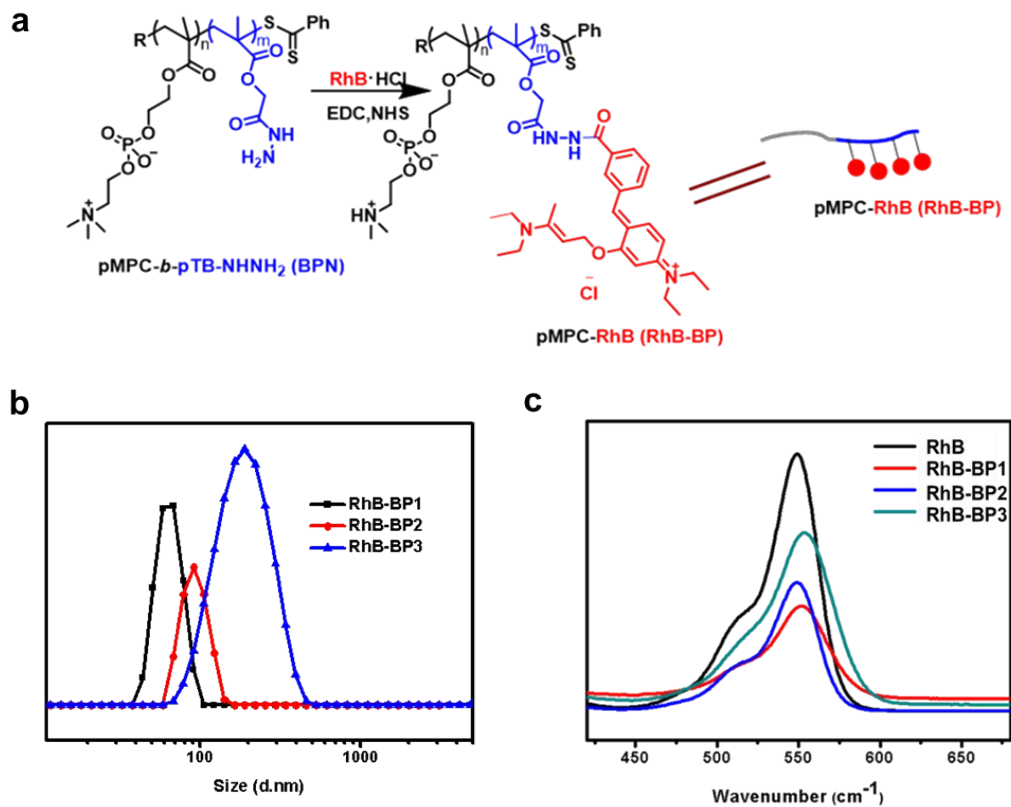


Figure S5: (a) Synthesis route of pMPC-RhB (RhB-BP). (b) DLS curves of RhB-BP1 (black line), RhB-BP2 (red line) and RhB-BP3 (blue line). (c) UV-vis spectrum of RhB-BP1 (red line), RhB -BP2 (blue line), RhB -BP3 (cyan line) and RhB hydrochloride (black line) in water.

Table S3. Characterization of RhB-BP NPs.

samples	RhB (wt %) ^a	Size (nm) ^b	Zeta (mV) ^c
RhB-BP1	12%	~64	-0.1
RhB-BP2	16%	~98	-0.2
RhB-BP3	19%	~200	0.05

^aRhB loading is obtained by UV-vis spectroscopy at 488 nm. ^bHydrodynamic diameter measured in water by DLS. ^cZeta potential measured in water by Zetasizer.

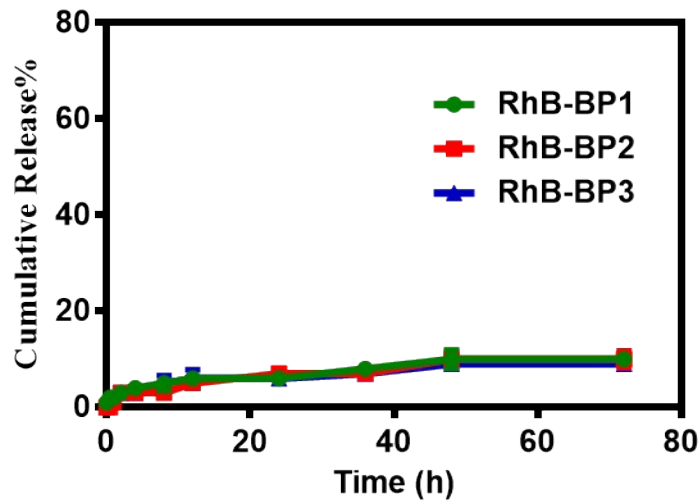


Figure S6: In vitro release curve of RhB from different RhB-BP NPs under pH=5.0 value (RhB-BP1: green line; RhB-BP2: red line; RhB-BP3: blue line).

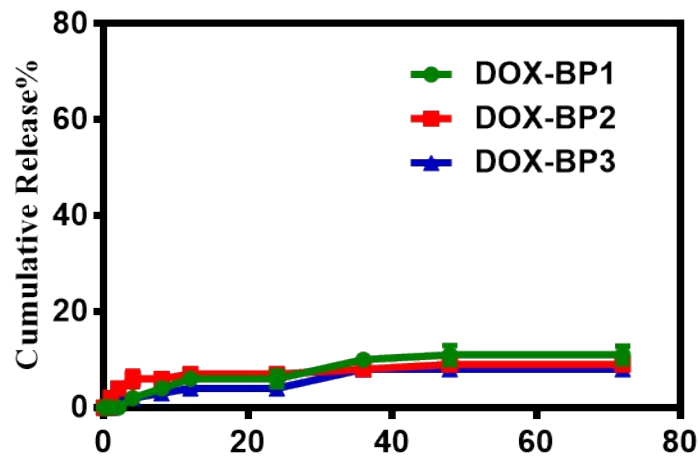


Figure S7: In vitro release curve of DOX from different sizes DOX-BP NPs under pH=7.4 value (DOX-BP1: green line; DOX-BP2: red line; DOX-BP3: blue line).

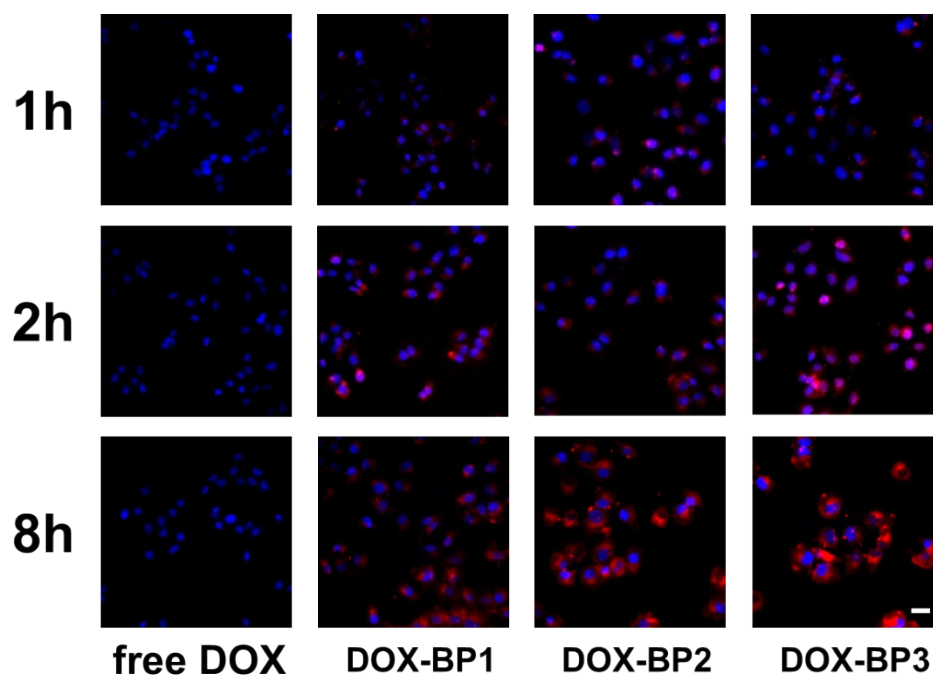


Figure S8: Fluorescence images of MCF-7/ADR cells incubated with free DOX, DOX-BP1, DOX-BP2 and DOX-BP3 for 1h, 2h and 8 h. Scale bars: 30 μm . All cells incubated with samples at a same DOX concentration (10 $\mu\text{g/mL}$).

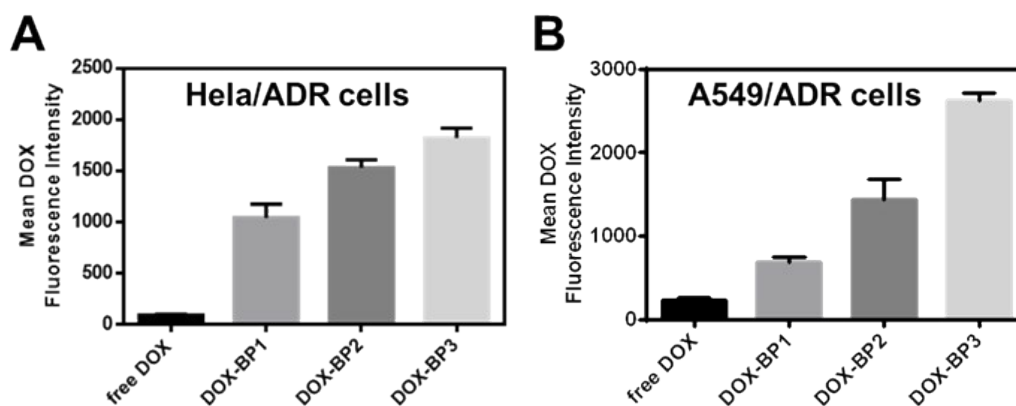


Figure S9. Fluorescence intensity in HeLa/ADR cells (A) and A549/ADR cells (B) after treatment free DOX and varisized DOX-BP NPs for 8 h. All cells incubated with samples at a same substrate concentration (DOX= 10 $\mu\text{g/mL}$).

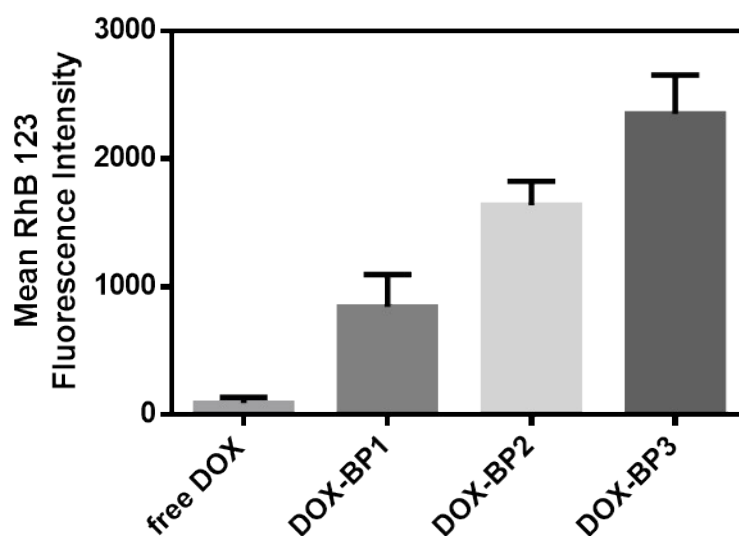


Figure S10. Corresponding fluorescence intensity in MCF-7/ADR cells after co-incubated with RhB123&free DOX or RhB123&different sizes DOX-BP NPs for 8 h. All cells incubated with samples at a same substrate concentration (DOX= 10 $\mu\text{g}/\text{mL}$, RhB123=10 $\mu\text{g}/\text{mL}$).

As shown in Figure S10, low intracellular RhB123 fluorescent intensity was observed in RhB123&free DOX-incubated cells, attributing to the inherently resistant to RhB123. Moreover, compared to RhB123&free DOX-incubated cells, high RhB123 fluorescent intensity could be observed in RhB123&DOX-BP NPs-incubated cells, and highest RhB123 fluorescent intensity could be observed in RhB123&DOX-BP3-incubated cells. These results revealed that the increase in size of DOX-BP NPs is able to increase the intracellular accumulation of other P-gp substrate (RhB 123), which is consistent with our conclusion.

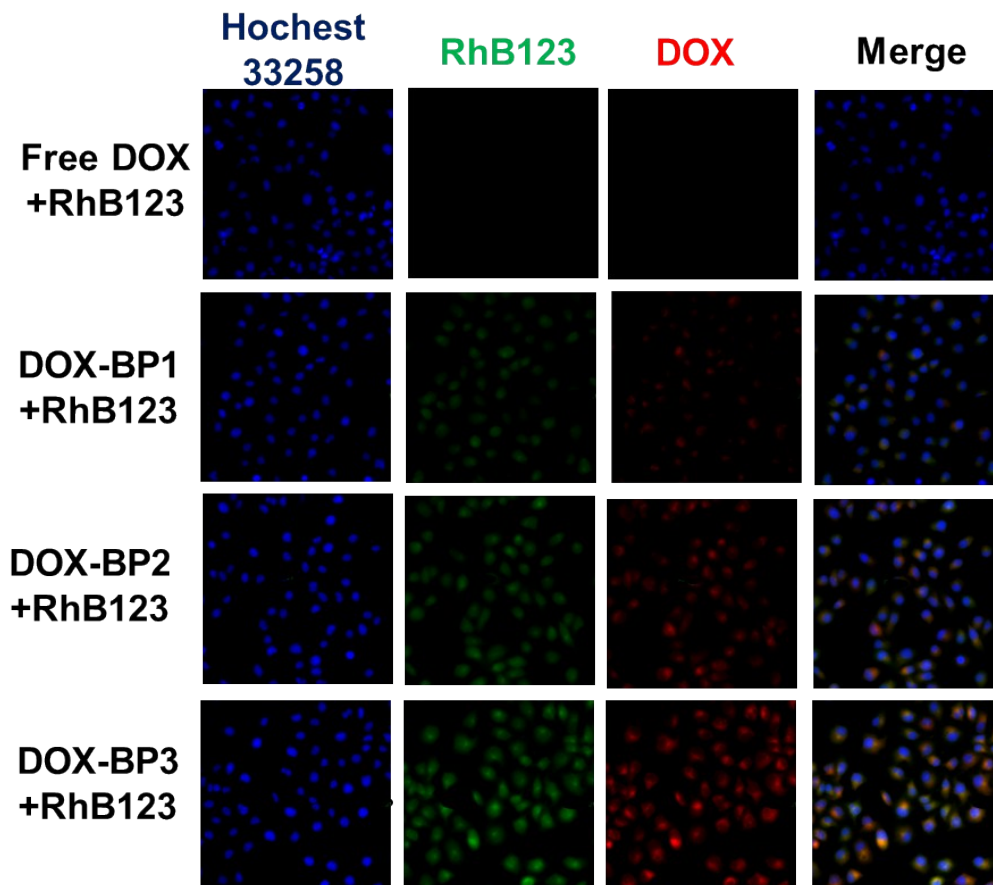


Figure S11. Fluorescence images of MCF-7/ADR cells after co-incubated with RhB123&free DOX or RhB&different sizes DOX-BP NPs for 8 h. Green fluorescence: RhB123. Scale bars: 30 μ m. All cells incubated with samples at a same substrate concentration (DOX= 10 μ g/mL, RhB123=10 μ g/mL).

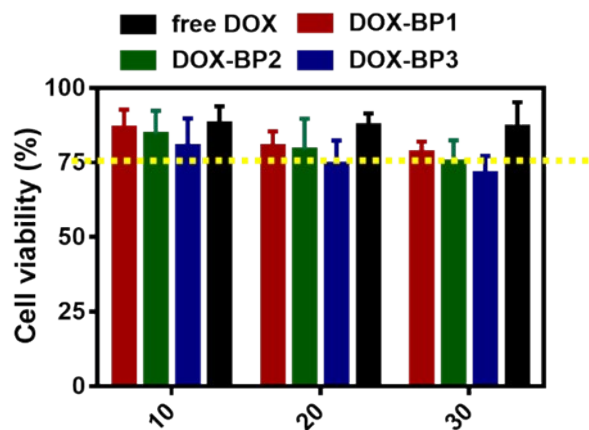


Figure S12: Cell viability of MCF-7/ADR cells treated with DOX-BP1, DOX-BP2, DOX-BP3 and free DOX (10, 20 and 30 µg/mL, DOX concentration) for 24 h.

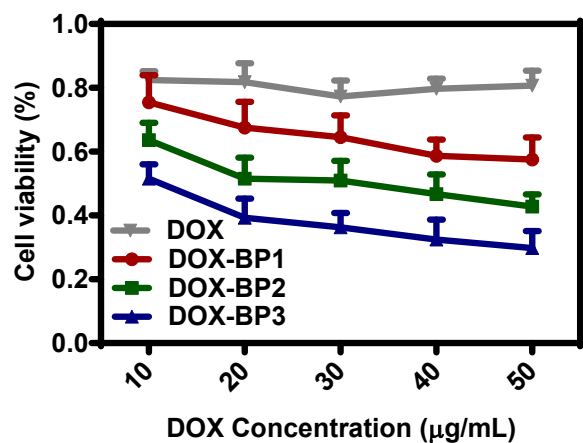


Figure S13: Cell viability of MCF-7/ADR cells treated with DOX-BP1, DOX-BP2, DOX-BP3 and free DOX (10, 20, 30, 40 and 50 µg/mL, DOX concentration) for 72 h.

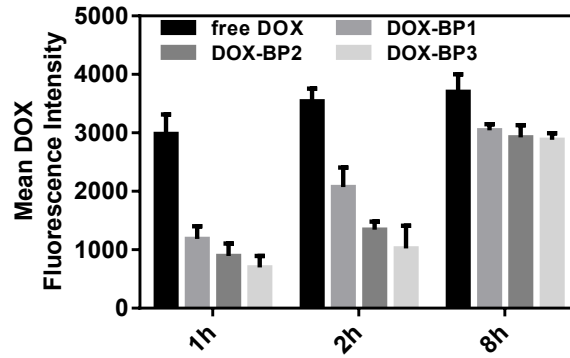


Figure S14: Corresponding fluorescence intensity in MCF-7 cells treatment with free DOX and varisized DOX-BP NPs for 8 h. All cells incubated with samples at a same drug concentration (DOX= 2 $\mu\text{g}/\text{mL}$).

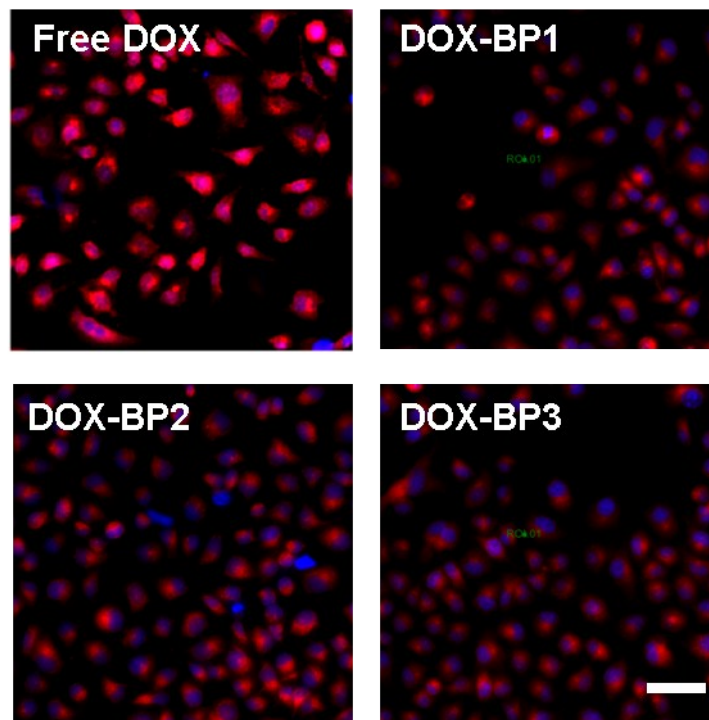


Figure S15: Fluorescence images of MCF-7 cells treatment with free DOX and varisized DOX-BP NPs for 8 h. All cells incubated with samples at a same drug concentration (DOX= 2 $\mu\text{g}/\text{mL}$). Red fluorescence: DOX. Scale bars: 30 μm .

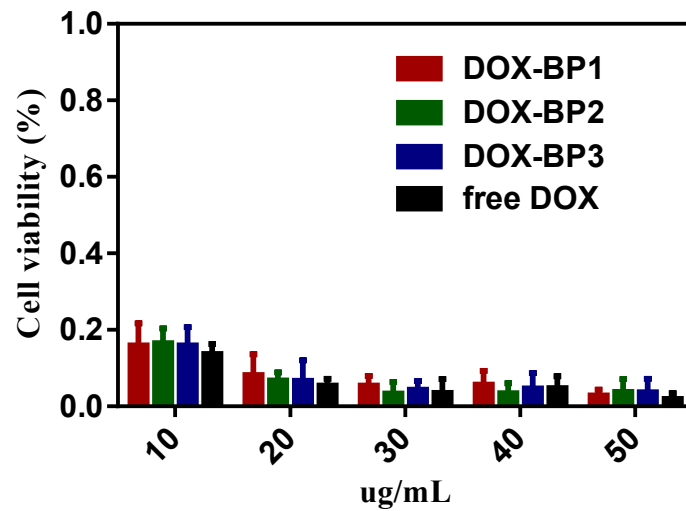


Figure S16: Cell viability of MCF-7 cells treated with DOX-BP1, DOX-BP2, DOX-BP3 and free DOX (10, 20, 30, 40 and 50 µg/mL, DOX concentration) for 24 h.

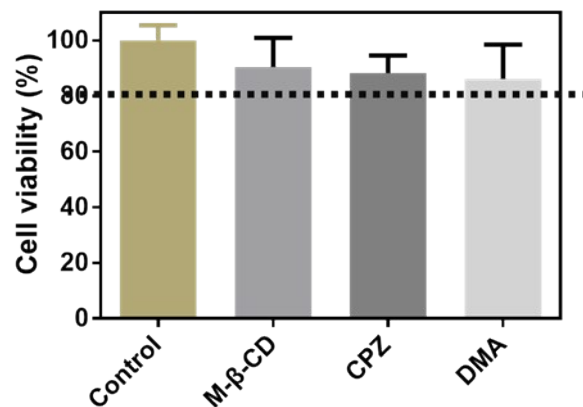


Figure S17: Cell viability of MCF-7/ADR cells treated with (Control: none, M-β-CD: 5 mg/mL, CPZ: 20 µg/mL, DMA: 10 µg/mL) for 4 h. Results are presented as mean ± SD (n=6).

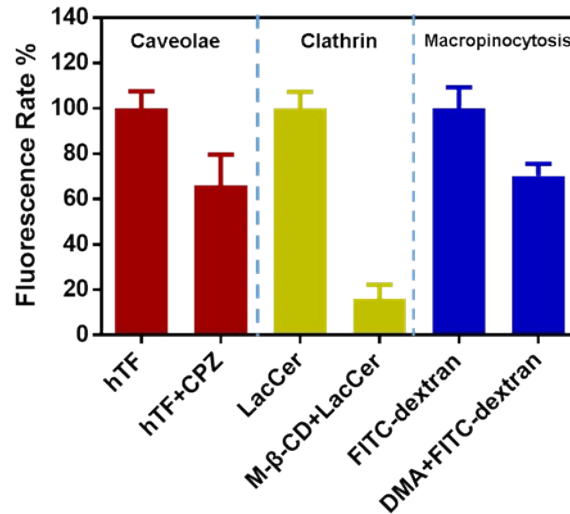


Figure S18: Fluorescence intensity of different inhibitory markers with cells that incubated with or without different specific inhibitor for 1 h. Inhibitory efficiency was investigated using fluorescently labeled endocytic markers, which are molecules known to be exclusively internalized via specific endocytic pathways. (lactosylceramide (LacCer) for clathrin-mediated endocytosis, human transferrin (hTF) for caveolae-mediated endocytosis and FITC-dextran for macropinocytosis).

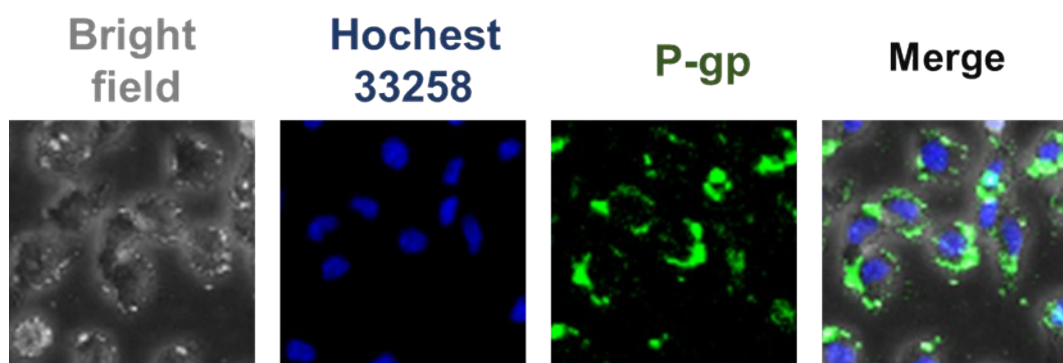


Figure S19. Fluorescence images of UIC2 labeling on surface P-gp of untreated MCF-7/ADR cells. Merge image shown the asymmetrical distribution of P-gp.